

APPLICATION OF SPACE SHUTTLE PHOTOGRAPHY TO STUDIES OF UPPER OCEAN DYNAMICS

Quanan Zheng, Vic Klemas, Xiao-Hai Yan, and Zongming Wang
Center for Remote Sensing, Graduate College of Marine Studies
University of Delaware, Newark, DE 19716

ABSTRACT

Three studies have been conducted using space shuttle imagery to explain the dynamics behavior of internal waves in the Atlantic and Indian Oceans and to derive tide-related parameters for Delaware Bay. By interpreting space shuttle photographs taken during mission STS-40, a total of 34 internal wave packets on the continental shelf of the Middle Atlantic Bight have been recognized. Using the finite-depth theory we derived that the maximum amplitude of solitons is 5.6 m, the phase speed 0.42 m/s, and the period 23.8 min. Deep-ocean internal waves in the western equatorial Indian Ocean on photographs taken during mission STS-44 were also interpreted and analyzed. The internal waves occurred in the form of a multisoliton packet in which there are about a dozen solitons. The average wavelength of the solitons is 1.8 ± 0.5 km. The crest lines are mostly straight and reach as long as 100 km. The distance between two adjacent packets is about 66 km. Using the deepwater soliton theory, we derived that the mean amplitude of the solitons is 25 m, the nonlinear phase speed 1.7 m/s, and the average period 18 min. For both cases, the semidiurnal tides are the principal generating mechanism. The tide-related parameters of Delaware Bay were derived from space shuttle time-series photographs taken during mission STS-40. The water area in the bay were measured from interpretation maps of the photographs. The corresponding tidal levels were calculated using the exposure time. From these data, an approximate function relating the water area to the tidal level at a reference point was determined. Then, the water areas of the Delaware Bay at mean high water (MHW) and mean low water (MLW), below 0 m, for the tidal zone, and the tidal flux were inferred. All parameters derived were reasonable and compared well with results of previous investigations.

INTRODUCTION

Since 1981 the United States has performed Space Shuttle missions. After 15 years of operations, a Space Shuttle Earth Observations Project (SSEOP) database has been set up. Among the photographs, about 75% represent the globally distributed coastal zone. The database has been made easily accessible to the research community (ref. 1).

Space shuttle photographs taken by the astronauts with hand-held cameras are suitable for the study of upper ocean dynamics due to the following advantages. The first is the visualization of the imagery of ocean features. The features were identified by human eyes then photographed with the camera adjusted for optimum performance. This method is unparalleled for other spaceborne remote sensing techniques, because it allows phenomena in the deep ocean far away from any satellite receiving station to be imaged with human intelligence. The second advantage is high spatial resolution, which is 20 - 30 m, much better than 1 km for NOAA/AVHRR images which are frequently used in oceanographic studies. The third is highly repeatable observation frequency, which can reach once a day for a short period. Sometimes a phenomenon might be photographed several times within a minute if the astronauts are interested in it. That provides a good opportunity for observation of time-dependent processes.

The Center for Remote Sensing at the University of Delaware has been engaged in the application of space shuttle photography to studies of upper ocean dynamics since 1991. We developed digitization, geometric correction, and image enhancement techniques for data processing, and applied spatial Fourier transforms to the spectral analysis of spatially periodical phenomena. We used space shuttle photographs for extracting parameters of internal waves on the continental shelf of the Middle Atlantic Bight and the western equatorial Indian Ocean, and for calculating tidal parameters of the Delaware Bay (ref. 2, 3, and 4). The major results are reviewed here.

* This work is supported by the ONR Optics Program through grant N00014-95-1-0065; the NASA Space Shuttle Application Program and partly supported by the NOAA Global Change Program through grant NA26AP0257-01. The space shuttle photographs are provided by S. Ackleson, P. E. La Violette and K. Lulla.

SPACE SHUTTLE PHOTOGRAPHS

The space shuttle photographs used in our studies were taken with the Aero Linhof Technika 45 camera for mission STS-40 and with the NASA-modified Hasseblad 500EL/M camera for mission STS-44. The specifications of photographs and the related information are summarized in Table 1.

Table 1. Specifications and Related Information of Space Shuttle Photographs Used in Our Studies

| Item | Parameters or Description | |
|--------------------------|--|--|
| Mission | STS-40 | STS-44 |
| Platform | | |
| Space shuttle | Columbia | Atlantis |
| Flight date | June 5 - 14, 1991 | Nov. 24 - Dec. 1, 1991 |
| Orbit altitude (km) | 287 | 361 |
| Inclination (degree) | 39 | 28.46 |
| Sensor | | |
| Camera | Aero Linhof Technika 45 | NASA-modified Hasseblad 500 EL/M |
| Lens | 250 mm Tele-Arlon f/5.6 | 250 mm CF sonnar f/5.6 |
| Incidence angle (degree) | 0 | 0 |
| Film | | |
| Type | Kodak color transparency (QX 868) | Kodak Ektachrome 64 color transparency |
| Sensitive spectrum | Visible | Visible |
| Resolution (lines/mm) | 50 | 50 |
| Size of a scene (sq in.) | 4 × 5 | 4 × 5 |
| Photographing time | June 8 and 10, 1991 | Nov. 28 - 30, 1991 |
| Spatial Resolution (m) | 23 (nadir) | 23 (nadir) |
| Applications | Shallow water internal waves Delaware Bay | Deepwater internal waves |

OBSERVATIONS OF OCEAN INTERNAL WAVES

Internal Waves on the Continental Shelf of Middle Atlantic Bight

The enlarged space shuttle photographs with a size of 30 × 40 square inches taken at 1518:24 and 1518:41 UT, or 1118:24 and 1118:41 EDST, June 8, 1991, were used for extracting the information of internal waves on the continental shelf of Middle Atlantic Bight. An interpretation map with geographic coordinates and sea bottom contours is shown in Figure 1. One can see that the total of 34 packets of internal waves are distributed over a huge area located from 38° to 40°N latitude and 72° to 75°W longitude, where water depth near the continental shelf break is from 50 to 150 m. The crest lines of internal waves are nearly parallel to local bottom contours, with the longest continuous length of 150 km. In this area, internal wave events have been observed with other satellites (ref. 5) and in situ investigations (ref. 6) many times in the last two decades. It is believed, therefore, that this is an active area for solitary internal waves.

The analysis of CTD data along the ship track AA shown in Figure 1 indicates that the case of interest satisfies the scale limits of the finite-depth theory. According to a steady state solitary solution given by Joseph (ref. 7), the amplitude of soliton has a form

$$A(\xi; a, b) = \frac{-\eta_0}{\cosh^2 a\xi + (\sinh^2 a\xi)/a^2 b^2} \quad (1)$$

where $\xi = x - Ct$, is a wavenumber like parameter ($= 2\pi/\lambda$) satisfying the relationship, $ab \tan(ah) = 1$, and

$$b = \frac{4h^2}{3\eta_0} \quad (2)$$

and C is the nonlinear soliton speed given by

$$C = C_0 \left\{ 1 + \frac{H}{2H} \left[1 + \frac{H}{b} (1 - a^2 b^2) \right] \right\}, \quad (3)$$

where C_0 is the phase speed of the lowest internal mode (ref. 8).

$$C_0 = \left(\frac{\delta\rho}{\rho} \frac{g}{k} \right)^{1/2} \left[\coth kh + \coth k(H-h) \right]^{-1/2}, \quad (4)$$

where k is the wavenumber. The characteristic scale, L , is defined by the value of ξ at which $A/\eta_0 = -1/2$, and is given by

$$aL = \cosh^{-1} \left[\frac{1 + 3(ab)^2}{1 + (ab)^2} \right].$$

We use equations (1)-(4) to calculate dynamic parameters of solitons.

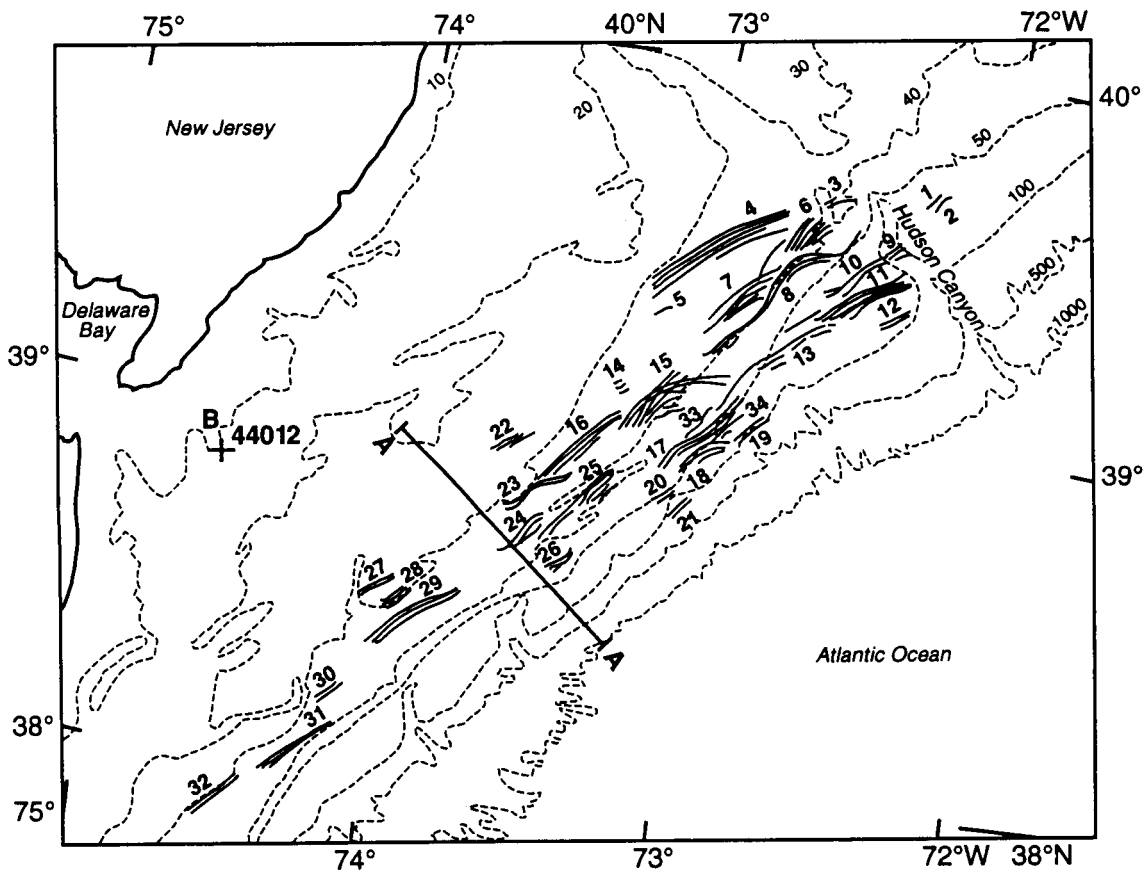


Figure 1. Internal wave interpretation map. The groups of solid lines coded with numbers are images of internal waves. The dashed lines are sea bottom contours with sounding in fathoms (1 fm = 1.8 m). Segment AA is the CTD data ship track; B marks the location of NOAA data buoy 44012.

Maximum amplitude. From (2) we have the maximum soliton amplitude $\eta_0 = 5.6$ m.

Soliton speed. From (4) we have $C_0 = 0.36$ m/s, and then from (3) we obtain the nonlinear soliton speed $C = 0.42$ m/s.

Period. From the characteristic wavelength and the phase speed we derive the characteristic soliton period $T = 23.8$ min.

Horizontal velocities of water particles in the upper and lower layers. For the upper layer,

$$U_1(x, t) = -U_{10} \operatorname{sech}^2[(x - ct)/L], \quad (5)$$

where $U_{10} = C_0 \eta_0 / h$. For the lower layer,

$$U_2(x, t) = -U_{20} \operatorname{sech}^2[(x - ct)/L], \quad (6)$$

where $U_{20} = C_0 \eta_0 / (H - h)$ (ref. 9). For our case we have $U_{10} = 0.13$ m/s, and $U_{20} = 0.030$ m/s.

Total energy per unit crest line. An estimate of the total energy per unit crest length is (ref. 9)

$$E = \frac{4}{3} (\rho_2 - \rho_1) g \eta_0^2 L. \quad (7)$$

For our case, we have $E = 6.8 \times 10^4$ J/m.

Deepwater Internal Waves in the Western Equatorial Indian Ocean

The space shuttle photographs taken during mission STS-44 were used for the study of deepwater internal waves in the western equatorial Indian Ocean. A map of the study area with space shuttle subtracks is shown in Figure 2. The isobaths

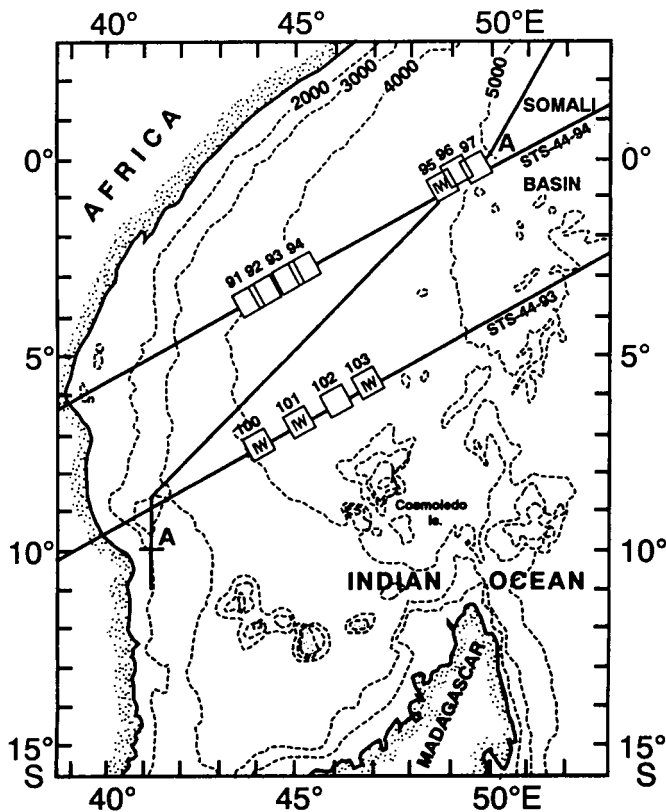


Figure 2. Map of the study area in the equatorial Indian Ocean. The parallel straight lines show subtracks of the space shuttle Atlantis during mission STS-44. Squares along subtracks show central locations and the coverage of space shuttle photographs. Numerals on the squares represent the number of each frame. IW in the squares denotes the photographs in which the internal waves are observed. Segment AA is the ship track for potential density measurements. Isobaths are in meters.

show that the depths of photographed locations range from 4000 to 5000 m, which are typical for the tropical deep ocean. Figure 3a shows one of the space shuttle photographs analyzed in this study coded STS 44-93-103. Its location and spatial coverage can be found in Figure 2. Figure 3b is an interpretation map of Figure 3a. One can clearly see the collision of two internal wave packets in the bottom center of the photograph. The images of the internal waves appear to be alternating bright and dark bands occurring in packets (see Figure 3a). The bands are nearly straight and have physical lengths as long as 100 km. The interpacket distance is 66.0 km. In a packet the number of waves may reach more than one dozen, and the wavelengths are distributed quite uniformly, unlike shallow-water internal wave packets in which the waves exhibit a general decrease in wavelength from the front to the rear of the packet (ref.10). The average wavelength is 1.8 ± 0.5 km.

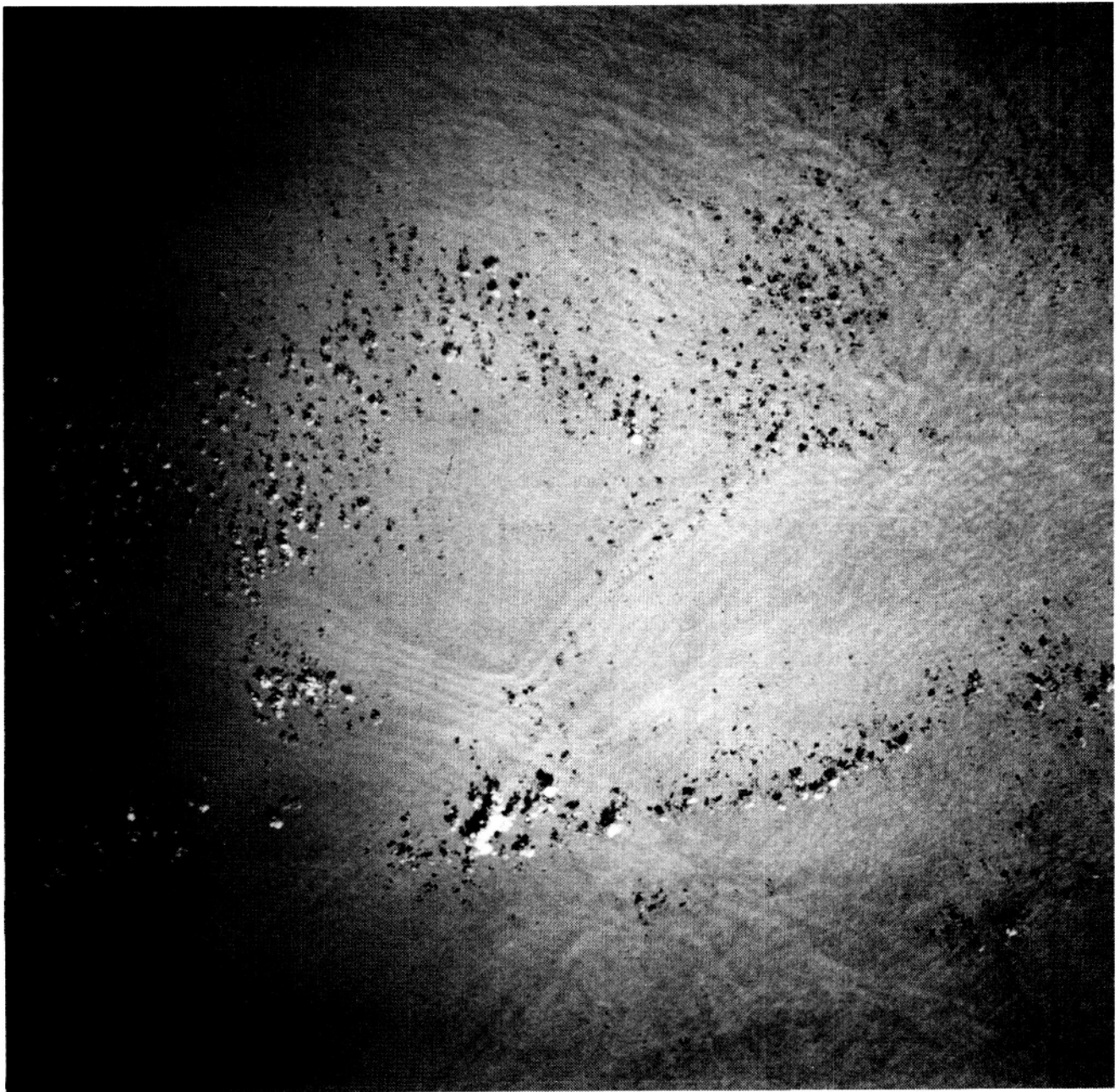


Figure 3a. Space shuttle photograph STS 44-93-103. Alternating bright and dark bands are surface manifestations of internal waves. The white and black spots are images of clouds and cloud shadows.

For the equatorial Indian Ocean, the vertical density structures can be quite accurately described by the two-layer model, with scale parameters: $h = 75$ m and $H = 4500$ m. Parameters L and η_0 are not directly measured quantities, but the following estimations are reasonable, that is, $L = O(0.3 \lambda) = O(5.4 \times 10^2$ m), and $\eta_0 = O(20$ m). These scale parameters indicate that our case is close to the conditions of deepwater theory. Using the Benjamin-Ono equation (ref. 11 and 12) and measurement data, we can obtain dynamic parameters of the internal waves as follows (ref.4).

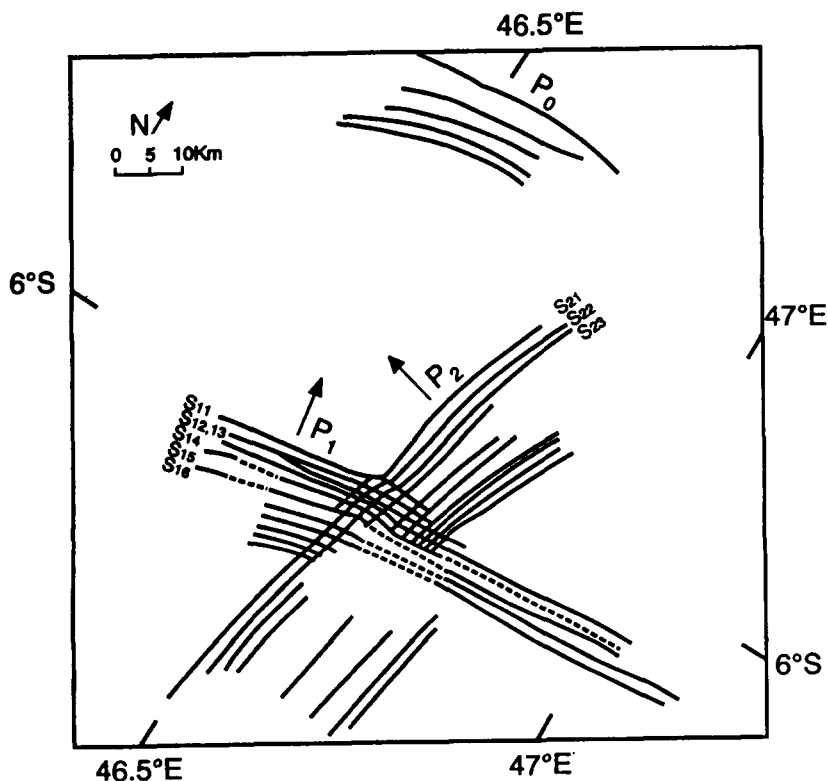


Figure 3b. Interpretation map of internal waves shown in Figure 3a.

Characteristic length. From space shuttle photographs, we have measured the average wavelength λ of 1.8 ± 0.5 km. Reasonably assuming that λ is the soliton width at one tenth of the amplitude (i.e., $\eta/\eta_0 = 0.1$), from mean conditions we derive the characteristic half-width of solitons $\Delta = 3.0 \times 10^2$ m. Therefore the characteristic length $L = 2\Delta = 6.0 \times 10^2$ m.

Amplitude. The amplitude of the solitons $\eta_0 = 25$ m.

Nonlinear phase speed. The average nonlinear phase speed of the solitons $V = 1.7$ m/s.

Period. From the average wavelength and nonlinear phase speed we derive the average period of the solitons $T = 18 \pm 5$ min.

Horizontal velocities of the water particles. Using the formula derived for the hyperbolic soliton (ref. 9), we can calculate the horizontal velocities of the water particles induced by the solitons. In the upper layer the average maximum horizontal velocity is

$$u_{10} = \frac{c\eta_0}{h} = 50 \text{ cm/s,}$$

and in the lower layer

$$u_{20} = -\frac{c\eta_0}{H} = -0.85 \text{ cm/s.}$$

One can see that the velocity of the water particles in the upper layer is quite large, but in the lower layer it is negligibly

small.

Total energy per unit crest length. The total energy per unit crest length of internal waves is approximately (ref. 8)

$$E = (\rho_2 - \rho_1) g \bar{\eta}^2, \quad (8)$$

where

$$\bar{\eta}^2 = \int_{-\infty}^{\infty} \eta^2(x,t) dx. \quad (9)$$

Calculating (9) and substituting the result into (8) yields the total energy per unit crest length

$$E = \frac{\pi}{2} (\rho_2 - \rho_1) g \eta_0^2 \Delta. \quad (10)$$

For our case, $\rho_2 - \rho_1 = 3 \times 10^{-3} \text{ g/cm}^3$, $\eta_0 = 25 \text{ m}$, and $\Delta = 3.0 \times 10^2 \text{ m}$, so that $E = 6.8 \times 10^6 \text{ J/m}$. We measured the separation distance between two adjacent packets, P_0 and P_1 , Λ , as being 66.0 km. The group speed $c_g = 1.5 \text{ m/s}$. Hence we derive that the period of internal wave packets $Tg = \Lambda/c_g = 12.2 \text{ hours}$. This result is close to the 12.5 hour average period of three most powerful modes of semidiurnal (M_2) tides in the study area.

DELAWARE BAY TIDAL PARAMETERS

The raw data used for this study are the positive color films with a size of $4 \times 5 \text{ sq. in.}$, which are dated June 8 and 10, 1991 during mission STS-40. The photographs are centered on Delaware Bay, and cover most of the coast of New Jersey, the Delmarva peninsula, and the Chesapeake Bay, as well as their adjacent continental shelf on the Middle Atlantic Bight. By enlarging the films into photographs with sizes $30 \text{ in.} \times 40 \text{ in.}$ and $16 \text{ in.} \times 20 \text{ in.}$, the basic images for mapping and surveying are produced.

Tidal Influx

According to the definition of the dynamics of a bay, the tidal influx, W_b , is calculated by

$$W_b = (S_1 + S_2) H / 2, \quad (11)$$

where S_1 and S_2 are the water areas corresponding to mean high water (MHW) and mean low water (MLW), respectively, and H is the mean tidal range, i.e. the difference in height between the two. This is a universal formula regardless of coastal geometry and bottom topography of the bay.

From (11), one can see that if S_1 , S_2 and H are known, the tidal influx, W_b can be calculated. Usually H can be found in the tide tables, and the areas S_1 and S_2 , must be measured either with a field survey or with remote sensing. Field surveys, however, hardly obtain synchronous data for a huge bay because of the changeable tide levels. Satellite remote sensing can provide synchronous imagery for a large bay, which can be used to map and to measure the water area. But the time of the satellite overpass rarely coincides with the required tide stage. In order to derive the water area at a given tide stage, it is necessary first to determine a function relating the water area to the tide level at a reference point. We assume that this function, $A(h)$, has the form of a power series:

$$A(h) = \sum_{n=0}^{\infty} k_n h^n, \quad (12)$$

where the variable h is the tide level at the reference point, and k_n the coefficient to be determined. Obviously, the water areas measured from satellite images, the exposure times and the tide tables can be used to obtain k_n , and the functional form of $A(h)$ can be determined. Then the water area of the bay at any tide level can be simply calculated. The accuracy of $A(h)$ determined by (12) depends on the highest order of h , n . If we have two groups of data of the water area and their corresponding tide levels, the coefficients k_0 and k_1 are obtained by solving coupled equations, and a linear equation of $A(h)$

can be determined as a first order approximation.

For this study, we chose two space shuttle photographs, which are coded 910608 151824 STS-40-LNHF-15 and 910610 135020 STS-40-LNHF-151-162, to determine the function of $A(h)$ for Delaware Bay. In these two photographs, the Delaware Bay is located near the central parts, and the geometric distortion of the imagery of the bay is relatively small, therefore, the measurement error due to this distortion is not significant. With the enlarged photographs, we prepared interpretation maps of the water areas in the Delaware Bay. The definition of the bay is as follows. The line between Liston Point, Delaware, and Hope Creek, New Jersey, is defined as the upstream limit of the bay, while that between the tips of Cape Henlopen and Cape May as the downstream one. And the two sides of the bay are bounded by boundaries of the sea water at exposure time. The scales of interpretation maps are determined using four reference points distributed on the two coastal sides of the bay. The distance between two reference points across the bay is derived from the Atlantic Coast map with a scale of 1:1,200,000 at Lat. 40°00'N published by the NOAA National Ocean Survey in 1975. Then the water areas are measured from interpretation maps with a CALCOMP 9100 digitizer and ERDAS Image Processing System. The resolution of this system is 0.01 cm², and measured areas in images are about 30 cm², therefore, measurement errors are negligible. For each map we made measurements three times. The mean and the standard deviation are

$$A(h_1) = (1720 \pm 5) \text{ km}^2 \text{ for the 910608 photograph}$$

and

$$A(h_2) = (1776 \pm 3) \text{ km}^2 \text{ for the 910610 photograph.}$$

Breakwater Harbor, located at the inside of Cape Henlopen (38°47'N, 75°06'W), is chosen as a reference point for the tide level. It is the only station in the Delaware Bay listed in the Tide Tables. The height of tide at exposure time is calculated according to the method given in Table 3 of the Tide Tables (ref. 13). Before the calculation was performed, the exposure times annotated in GMT on the photographs, were first transformed into the local time which is used in the Tide Tables. For the 910608 image, the local exposure time is 10:18:24 ET, and the tide level, h_1 , is 6 cm; for the 910610 image, 8:50:20 ET, and h_2 , 99 cm.

Substituting the values of $A(h_i)$ and h_i into (12), we obtain a linear function of the water area in the Delaware Bay versus the tide level at the Breakwater Harbor

$$A(h) = k_1 h + k_0 \text{ (km}^2\text{)} \quad (13)$$

where $k_1 = 0.60 \text{ km}^2/\text{cm}$, and $k_0 = 1717 \text{ km}^2$.

From the levels of high and low water at the Breakwater Harbor listed in the Tide Tables, we derive that the level of MLW is 3 cm, and that of MHW is 131 cm. Substituting these heights (levels) into (13), we have $S_1 = 1796 \text{ km}^2$, and $S_2 = 1719 \text{ km}^2$. The mean tidal range, H , in (11) can not be replaced directly with the values at Breakwater Harbor because it is variable along the coast. We chose 9 tidal stations which are generally uniformly distributed along both sides of the bay and coded by 1, 2, 3, 4, 9, 10, 11, 12 and Cape May Point shown in Figure 4 to take the average of the mean tidal ranges. We obtain the average $H = 1.57 \text{ m}$. Substituting S_1 , S_2 and H into (11), the tidal influx into Delaware Bay, W_b is derived as $2.76 \times 10^9 \text{ m}^3$. The uncertainty or error of this value is dependent on the accuracies of S_1 , S_2 and H . We believe that the error of this estimation is less than 3%, and is mainly caused by the interpretation error.

Tidal Zone Area

As a first order approximation, (13) can be used to calculate the area of the bay at any tide stage. As an example, we calculate the area of the tidal zone in Delaware Bay. Checking the Tide Tables, we find that the highest high water and the lowest low water at Breakwater Harbor in a year are 174 cm and -27 cm, respectively. With (13) their corresponding water area is calculated as 1821 km^2 , and 1701 km^2 , respectively. Based on that, we obtain the area of the tidal zone in the Delaware Bay $A_{int} = 120 \text{ km}^2$.

Area Below 0 m

If we let H in (13) be zero, we obtain the area below zero-meter depth for Delaware Bay, which is another important

parameter for a tidal bay $A_0 = 1717 \text{ km}^2$. This parameter characterizes the basic and stable part of the bay. If this parameter is getting smaller, that means that the bay is silting in.

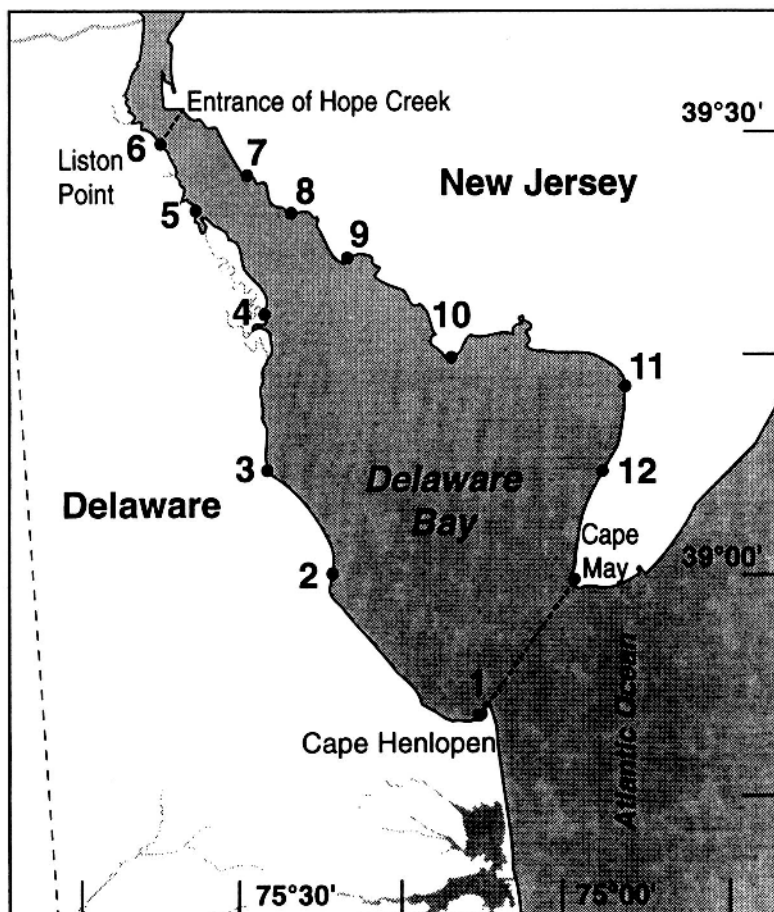


Figure 4. Interpretation map of the Delaware Bay drawn from the space shuttle photograph. The upstream and the downstream limits of the bay are drawn with the dashed and dotted lines. The solid circles coded along the coastal lines are the tide stations, for which historical data are available.

DISCUSSION AND CONCLUSIONS

1. The internal wave field on the continental shelf of the Middle Atlantic Bight has a three level structure which consists of packet groups, packets, and solitons. From photographs we measured an average packet group wavelength of 17.5 km and an average soliton wavelength of 0.6 km. Using the finite-depth theory, we derived dynamic parameters of internal solitons: the maximum amplitude, 5.6 m; the phase speed, 0.42 m/s; the period, 23.8 min; the amplitude of the velocity of the water particles in the upper and lower layer, 0.13 m/s and 0.030 m/s, respectively; and the total energy per unit crest line, $6.8 \times 10^4 \text{ J/m}$.

2. Like in the shallow-water case, deepwater internal waves occur in packets or groups, but the average number of individual waves in a packet reaches 12, which is more than the average of the shallow-water internal wave packet, i.e. four to six (ref. 3 and 9). The amplitude of 25 m, the nonlinear phase speed of 1.7 m/s, the maximum horizontal velocity in the upper layer of 0.5 m/s, the crest length of 100 km, and the total energy per unit crest length of $6.8 \times 10^6 \text{ J/m}$ indicate that deepwater internal waves are much stronger than those on continental shelves (ref. 3) and are similar to those in marginal seas, like the Andaman Sea (ref. 9).

3. The results of this study indicate that space shuttle photographs are valuable for studying bays and estuaries, not only qualitatively, but also quantitatively. High spatial resolution and small geometric distortion of the central parts of photographs provide a satisfactory accuracy for bay-scale mapping and measurement. Exposure time annotations on the photographs provide an important factor for calculating coincident tide levels which are a dominant forcing process in a bay originating

from the ocean. Combining these two directly measured parameters makes it possible to derive tide-related parameters of the bay, which are necessary for research and monitoring, but not easily obtained with traditional field surveys.

4. The water area at the Mean High Water (MHW) of the Delaware Bay is 1796 km², which is smaller than the historical value of the total surface area of 1864 km² or 720 square miles (ref. 14). The reason is different definitions for the bay. We use the legal definition of the bay which takes Liston Point as the upstream limit, and the line between the tips of Cape Henlopen and Cape May as the downstream limit of the bay, because these two reference points are easily recognized on space shuttle photographs. The historical data was calculated with the Smyrna River as the upstream limit and a fold line between Cape Henlopen and the southwest tip of Cape May as the downstream limit (see Fig. 3, in ref. 14). The area of a tidal zone of 120 km², and the area below the zero-meter level of 1717 km² obtained in our study are new results.

REFERENCES AND NOTES

1. Ackleson, S.G., A summary of hand-held ocean and coastal photography taken during space shuttle missions: 1981-1991 (Abstract), *EOS* 72, 1992, pp. 69.
2. Zheng, Q., X.-H. Yan, and V. Klemas, Derivation of Delaware Bay tidal parameters from space shuttle photography, *Remote Sens. Environ.*, 45, 1993, pp. 51-59.
3. Zheng, Q., X.-H Yan, and V. Klemas, Statistical and dynamical analysis of internal waves on the continental shelf of the Middle Atlantic Bight from space shuttle photographs, *J. Geophys. Res.*, 98, 1993, pp. 8495-8504.
4. Zheng, Q., V. Klemas, and X.-H. Yan, Dynamic interpretation of space shuttle photographs: Deepwater internal waves in the western equatorial Indian Ocean, *J. Geophys. Res.*, 100, 1994, pp. 2579-2589.
5. Sawyer, C., Tidal phase of internal-wave generation, *J. Geophys. Res.*, 88, 1983, pp. 2642-2648.
6. Burrage, D. M. and R. W. Garvine, Supertidal frequency internal waves on the continental shelf south of the New England, *J. Phys. Oceanogr.*, 17, 1987, pp. 808-819.
7. Joseph, R. I., Solitary waves in a finite depth fluid, *J. Phys. A math. Gen.*, 10, 1977, pp. L225-L227.
8. Phillips, O. M., The dynamics of the upper ocean, 2nd ed., *Cambridge University Press.*, New York, 1977, pp. 336.
9. Osborne, A. R. and T. L. Burch, Internal solitons in the Andaman Sea, *Science*, 208, 1980, pp. 451-460.
10. Apel, J. R. and F. I. Gonzalez, Nonlinear features of internal waves off Baja California as observed from the SEASAT imaging radar, *J. Geophys. Res.*, 88, 1983, pp. 4459-4466.
11. Benjamin, T. B., Internal wave of permanent form in fluids of great depth, *J. Fluid Mech.*, 29, 1967, pp. 559-592.
12. Ono, H., Algebraic solitary waves in stratified fluids, *J. Phys. Soc. Jpn.*, 39, 1975, pp. 1082-1091.
13. U.S. Department of Commerce, NOAA/NOS, *Tide Tables 1991*, East Coast of North and South America including Greenland, 1990, pp. 239-241.
14. Polis, D. F., and S. L. Kupferman, *Physical Oceanography*, Delaware Bay Report Series, Vol. 4, University of Delaware, Newark, 1973, pp. 1-143.